JOURNAL OF CATALYSIS 136, 59–75 (1992)

Methanol Synthesis from H_2, CO, and CO_2 over Cu/ZnO Catalysts

K. G. CHANCHLANI,[1] R. R. HUDGINS, AND P. L. SILVESTON[2]

Department of Chemical Engineering, University of Waterloo, Waterloo, Ontario, Canada N2L 3G1

Received October 10, 1991; revised January 22, 1992

Methanol synthesis kinetics at steady state are reported for two catalysts: Cu/ZnO (as Cu : Zn = 30 : 70 atomic ratio) and $Cu/ZnO/Al_2O_3$ (Cu : Zn : Al = 60 : 30 : 10 atomic ratio) for various syngas compositions and temperatures from 200 to 275°C. In addition, catalyst deactivation is discussed along with XPS–Auger measurements of surface composition for fresh and used catalysts. Apparent activation energies for methanol synthesis on the Cu/ZnO catalyst depend on both temperature and fractional CO_2 in the CO–CO_2 mixture and reflect a change in the importance of the CO and CO_2 as sources of methanol in the synthesis. The water–gas shift reaction does not proceed to equilibrium for CO mole fractions below 0.05. Experimental results confirm earlier observations that methanol is formed directly from CO and CO_2. However, in syngas mixtures, methanol production from CO and CO_2 is not just additive; some interconversion must be involved.

INTRODUCTION

Research on the controversial role of CO_2 in methanol synthesis and the mechanism of its synthesis has centered recently on sophisticated instrumental techniques, such as isotopic methods (*1–7*); temperature-programmed reaction (*8*); surface spectroscopy such as XPS, Auger, and EXAFS (*8–12*); TPD (*13–15*); chemical trapping (*16–18*); IR or UV spectroscopy (*19–23*); and N_2O titration (*12, 24*). These studies have not settled the controversy. Many of these instrumental and/or technique-oriented studies also reported limited kinetic data on the role of CO_2 in the synthesis. Nevertheless, the primary source of kinetic data for studying the role of CO_2 are four extensive but apparently conflicting studies by Klier *et al.* (*25*), Vedage *et al.* (*2*), Rozovskii *et al.* (*26*), and Liu *et al.* (*27*). Klier and co-workers found that CO_2 activates Cu/ZnO catalysts at low concentrations or R ratios (R is the fraction of CO_2 in the carbon oxide portion of the feed) but inhibits formation of methanol (MeOH) at higher R ratios. On the other hand, Kung and co-workers (*27*) observed an increasing rate of response as R increased. Others (*4, 28, 29*) besides Liu *et al.* (*27*) have reported that the rate of CO_2 hydrogenation to methanol is much greater than the rate of CO hydrogenation. It seems appropriate, therefore, to investigate the role of CO_2 to supplement the kinetic measurements of the Klier and Kung teams as well as other investigators.

The results reported in this paper are drawn from an examination of periodic operation of methanol synthesis (*30*) in which the partial pressures of H_2, CO, and CO_2 were varied with time. Interpreting the periodic results requires an extensive collection of steady-state data. These data are the substance of this paper. Methanol synthesis kinetics are reported for two catalysts: Cu/ZnO (as Cu : Zn = 30 : 70 atomic ratio) and $Cu/ZnO/Al_2O_3$ (Cu : Zn : Al = 60 : 30 : 10 atomic ratio). The former was used by both Kung and co-workers and by Klier and co-workers, whereas the latter is the approximate composition of a widely used industrial methanol catalyst (*4*). The Klier group worked at 5 MPa and 225 to 250°C with $0 < R < 0.3$, whereas Kung and co-workers

[1] Present address: SACDA Inc., 343 Dundas St., Suite 500, London, Ontario, Canada N6B 1V5.

[2] To whom correspondence should be addressed.

0021-9517/92 $5.00

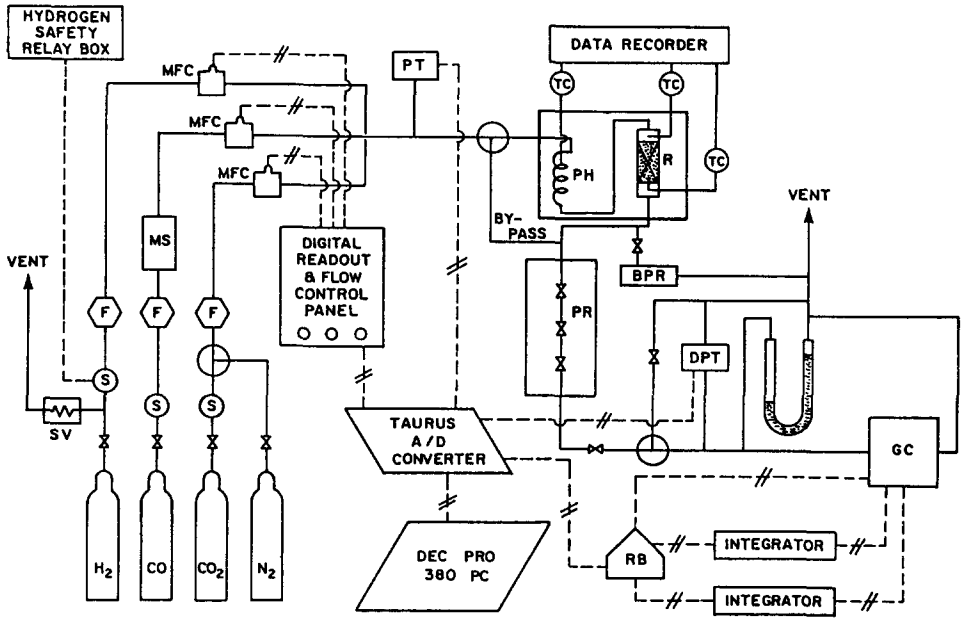

FIG. 1. Schematic of the experimental system: BPR, back pressure regulator; DPT, differential pressure transducer; F, microfilter; GC, gas chromatograph; MFC, mass flow controller; MS, molecular sieve bed; PC, microcomputer; PH, preheater; PR, pressure reducing valve; RB, relay box; S, solenoid valve; SV, safety valve; TC, thermocouple.

operated at 1.75 MPa and 198 to 228°C with $0 < R < 1$. Both groups used 70 mol% H_2. In addition to the kinetic measurements, catalyst deactivation, as well as XPS–Auger measurements of surface composition, is reported.

EXPERIMENTAL

Experimental System and Procedure

A schematic of the apparatus used in this study is shown in Fig. 1. High-pressure gases, CP grade CO (99.5%), instrument grade CO_2 (99.99%), and prepurified H_2 were used to avoid a booster compressor. Each of these gases passed through a high-pressure microfilter to eliminate dust and the CO stream was directed through a bed of 4A molecular sieves to strip out iron and/or nickel carbonyls. As shown in the figure, the composition of the feed gas was formulated using Brooks Model 5850D mass flow controllers (MFCs). The CP grade CO contained trace quantities of methane whereas nitrogen was the major contaminant in CO_2 and H_2.

By means of a three-way switching valve, the feed mixture could be sent either to the reactor or directly to an on-line gas chromatograph (GC) for feed composition analysis. The product analysis of the effluent stream from the reactor was initiated and controlled by an automated DEC PRO-380 microcomputer connected to various field devices via a Taurus One interface. The individual MFCs and the entire reactor were under supervision of the automated data acquisition system. Solenoid valves were employed on each stream to shut off the flow of gas completely when required.

A differential packed-bed reactor was used for the study. Constructed from a 0.635-cm (1/4-in.). o.d. copper tubing, the reactor was filled to a depth of about 3 cm with catalyst. Two chromel–alumel thermocouples were used to measure the temperature of the feed gas at the inlet to the catalyst

bed. The reactor operated virtually isothermally in all the steady-state runs reported. Total flow through the reactor was maintained at 14.8 ml (STP) s^{-1}. The catalysts described below were ground to 40/60 US mesh with a mean particle size of 0.3 mm. The charge was diluted with nonporous glass beads in a mass ratio of 1:2 (beads: catalyst) to distribute the heat generation and thereby maintain an isothermal condition in the reactor. The reactor was housed in a rectangular, aluminum, electrically heated furnace where temperature could be held to within 0.3°C of the desired level. A separate preheater raised the feed temperature to within 5°C of the temperature within the reactor. The reactor outlet led to a backpressure regulator, which served to maintain the total pressure at 2.86 MPa. The pressure drop across the catalyst bed was less than 5 kPa. After the backpressure regulator, the product stream passed into the sampling valve of the gas chromatograph. The gas chromatograph employed 80/100 mesh Porapak Q packing. Both thermal and flame ionization detectors in series provided the analysis at a maximum frequency of a measurement every 4 min. Integration was online. A mixture of 8.5% H_2 in He was used as a carrier gas to resolve the hydrogen peaks. Calibrations were performed for methanol, CO, and CO_2, whereas the response factor method (*31*) was used for water and methane. Further details of the equipment and analytical technique are given by Chanchlani (*30*).

Catalyst

The composition and preparation of industrial methanol catalysts are for the most part proprietary information. Samples are not readily available. Consequently, Cu/ZnO and Cu/ZnO/Al_2O_3 catalysts were prepared for this study following the recipes given by Klier and Herman (*32*). Once the catalyst charge was loaded into the reactor, it was conditioned by passing 15% H_2 in N_2 over the catalyst at high throughput for 10 h at 250°C and 101.3 kPa. When an experiment was not in progress, the reactor temperature was maintained, but the catalyst was continuously flushed with N_2.

TABLE 1

Catalyst Properties

Catalyst	Cu/ZnO (30/70)	Cu/ZnO (30/70)	Cu/ZnO/Al_2O_3 (60/30/10)
Composition			
Cu	30.97	30.82	60.51
Zn	69.03	68.18	30.90
Al	—	—	8.58
BET surface area (m^2 g^{-1})	40	30	54
Mean pore diameter (nm)			4 – 4.5
Internal porosity	0.45	0.45	0.45
Bulk density (g ml^{-1})	1.2	1.2	0.9
Mean particle diameter (mm)	0.3	0.3	0.3

The Cu/ZnO and Cu/ZnO/Al_2O_3 catalysts were chosen on the strength of having the highest activity for the two- and three-component catalysts for methanol synthesis, according to Klier and Herman (*32*). The composition of the Cu/ZnO/Al_2O_3 is virtually identical to a widely used industrial catalyst (*4*) while the Cu/ZnO catalyst has been used for many laboratory studies.

Nominal compositions of the catalysts prepared were determined by atomic absorption spectrophotometry and are given in Table 1. BET surface areas and mean pore radii from N_2 physisorption are also shown.

Experimental Procedure

Blank runs at 225 and 275°C at 2.86 MPa pressure with a H_2/CO/CO_2 feed (= 70/23/07 mol%, hereafter understood to be simply %) established that the glass beads, reactor walls, and stainless-steel supporting screen for the catalyst were catalytically inactive.

The activity of both catalysts decayed slowly during the runs. No attempt was made to regenerate the catalyst. There was also some variability in the catalyst activity

from batch to batch, so only data from samples with essentially the same initial activity are reported. The catalyst activity was monitored every 3 or 4 runs at 250°C and 2.86 MPa with a standard feed gas mixture (H_2/CO/CO_2 = 70/23/07). All of the methanol steady-state reaction rates were corrected to a common initial activity for each of the two different catalysts. These corrected data are reported. This technique requires the inspection of reproducibility, which was performed several times using a set of three to five replicated experiments.

Tests were undertaken for heat and mass transport interference employing various criteria (for gradients of temperature and concentration within the catalyst and within the film surrounding it) proposed in the literature (*33*). All of these tests were strongly negative, indicating the absence of transport masking. From these calculations, particle sizes and gas flow rates at which masking would be eliminated were selected, and these conditions were used in subsequent experiments. In addition, catalyst dilution (as already mentioned), reactor diameter, and the ratio of particle to reactor diameters were chosen to ensure isothermality.

Conversions based on carbon were, for the most part, less than 1%, establishing that the reactor operated differentially. Furthermore, the molar gas flow rates were practically unchanged. This permitted correlation of rates and yields with inlet conditions.

Material balances were made for carbon and oxygen. These closed to within about 2% for the experiments reported in this paper. Replication runs provided a coefficient of variability (standard deviation/mean rate of reaction) of from 4 to 27% for the experiments made with a Cu/ZnO catalyst and from 5 to 29% for the experiments made with a $Cu/ZnO/Al_2O_3$ catalyst. The mean coefficient of variation was about 14%. Furthermore, the approach to steady state was closely monitored at each steady state and it was observed that 120 to 150 min were needed to obtain time-invariant compositions.

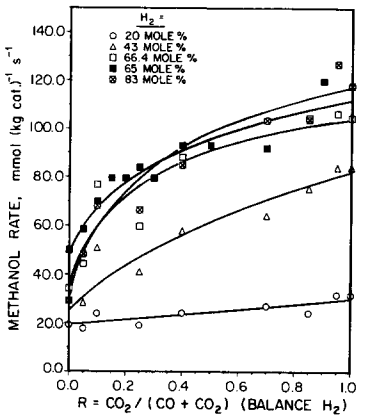

FIG. 2. Methanol synthesis rate as a function of R and % H_2. Feed contains CO, CO_2, and H_2; T = 225°C; P = 2.86 MPa; flow = 14.8 ml (STP) s^{-1}; Cu/ZnO catalyst.

Experiments were performed at 225°C, 2.86 MPa, and a space velocity of about 37 ml (STP) (g cat.)$^{-1}$ s^{-1} unless otherwise noted. The hourly space velocity at reaction conditions was between 8500 and 11,300 h^{-1}.

RESULTS

Experiments are separated by catalyst and arranged in the sequence

(1) effects of R and H_2 mole percentage on the synthesis rate,

(2) effect of H_2 mole fraction on the synthesis rate for $CO–H_2$ and $CO_2–H_2$ mixtures,

(3) effect of temperature on the synthesis rate, and

(4) catalyst deactivation and surface analysis.

Cu/ZnO Catalyst

Kinetics. For the Cu/ZnO catalyst, the experimental measurements are plotted in Fig. 2 as the rate of methanol formation vs R, where R is the fraction of CO_2 in the carbon oxide feed to the reactor. The rates are shown for different mole percentages of hydrogen in the feed. All results are for a temperature of 225°C and a total pressure of

2.86 MPa. At low % H_2, the rate of methanol formation seems to be independent of R, whereas by 43% H_2, the rate has become a strong function of R, as seen in Fig. 2. The curves for 66.4, 65, and 83% H_2 are in general agreement with the results obtained by Kung and co-workers (*27*) who observed a linear relation between rate and R in the range $0.1 < R < 1.0$ that they studied at 70% H_2. However, their rates (*27*) were about two orders of magnitude below those given in Fig. 2. This difference reflects total pressure, catalyst conditioning, and correction for deactivation. It is worthy of note that at high values of R and hydrogen content (>66%), the rate again appears to be weakly affected by R. We believe this is not a consequence of the water–gas shift reaction. Neither does it appear to represent water inhibition. Vedage *et al.* (*2*) report water inhibition at ca. 2% water in the exit gas, while Liu *et al.* (*27*) show strong inhibition below 1%. Water measurements in this study were poorly reproducible but were nevertheless below 1% as carbon conversion to methanol exceeded 1% only at 83% H_2 in the feed.

Explanations of the positive effect of R on the methanol formation rate go to the heart of the controversy over the role of CO_2, namely:

(1) CO_2 functions only to control the surface composition, oxidation state, and dispersion of CuO in the catalyst but is not a direct reactant.

(2) Methanol is formed solely through CO_2 hydrogenation.

(3) Both CO and CO_2 can be hydrogenated to methanol and the predominant reaction depends on operating conditions.

An increase in sites and/or the turnover number at each site is supported by the observations of Chinchen *et al.* (*13*). In a comprehensive review, Klier *et al.* (*25*) cite the pre-1982 evidence for a primarily CO route to methanol and argue for this route based on their studies of the effect of R on the synthesis rate (*25*). The arguments supporting the second viewpoint are summarized

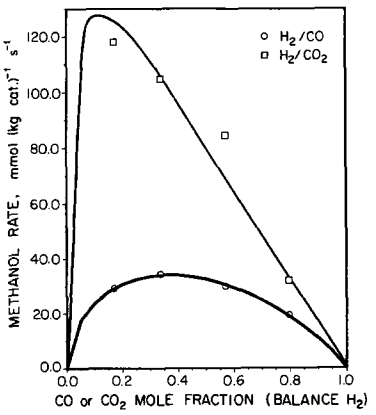

FIG. 3. Methanol synthesis rate for CO/H_2 and CO_2/H_2 feeds. T = 225°C; P = 2.86 MPa; flow = 14.8 ml (STP) s^{-1}; Cu/ZnO catalyst.

by Chinchen *et al.* (*34*). The third explanation is supported by most recent experimental data (*1, 4, 7, 20, 24, 26, 27*).

At low hydrogen concentrations (20% H_2), the R effect disappears. Neither of the two explanations can account for this behavior. Perhaps the hydrogen concentration on the surface becomes so small that hydrogen replacement becomes rate-limiting, thereby decreasing the influence of the CO/CO_2 ratio on the rate. Monnier *et al.* (*11*) proposed that the chemisorption of the carbon oxides is competitive with hydrogen. If hydrogen is capable of adsorbing on the same site, this explanation becomes reasonable. In another paper, Klier *et al.* (*25*) report that the heats of adsorption, and thus the strength of the adsorption bonds, decrease in the order $CO_2 > CO > H_2$. Duprez *et al.* (*7*) suggest that ZnO activates both CO_2 and H_2, so this could be the source of the interference. According to the formyl mechanism, now thought to be an intermediate in the CO route, atomically adsorbed H is needed. Formate, the apparent intermediate in the CO_2 route, is formed by the interaction of adsorbed H_2 and CO_2.

The two explanations can be evaluated by comparing in Fig. 3 the methanol formation rates for a feed containing only CO and H_2

and another containing only CO_2 and H_2. In this figure, the methanol formation rate at a mixture of 10% carbon oxides and 90% H_2 is five times greater for CO_2 than it is for CO. The reverse water–gas shift does not go to equilibrium (see Discussion). Even if it does proceed, this shift cannot explain the rate difference. The CO/CO_2 equilibrium ratio is about 1 (corresponding to $R = 0.5$). From Fig. 2 at $R = 0.5$, the rate would be about 100 mmol (kg cat.)$^{-1}$ s^{-1}. This rate is still well above the H_2/CO curve in Fig. 3. Since the CO/H_2 mixture cannot undergo the water–gas shift when water is not present, the assumption that the reaction proceeds only through CO requires an unlikely fourfold increase in the turnover number of density of active sites due to the presence of CO_2 in order to reach the 100 mmol (kg cat.)$^{-1}$ s^{-1} rate required at $R = 0.5$ in Fig. 2. Thus, the data in Figs. 2 and 3 suggest that methanol is formed in separate reaction pathways from CO and from CO_2.

Small amounts of methane were detected in the experiments when CO was part of the feed mixture. However, it was observed that methane concentration was nearly a linear function of the CO content. With just CO_2 and H_2, methane was not observed in the products. Thus, it appears that methane is not formed over this catalyst. This was confirmed by measuring the methane content of the CO cylinders after the experiments. It was determined that most of the methane originated with the CO feed. Water was measured when CO_2 was present in the feed mixture. No water was found when the feed contained only CO and H_2. Conversions were very low in these experiments so that the water content in the product was at the limit of detection by the TCD determination. The reproducibility and accuracy of the water measurements were consequently quite low. Indeed, in some cases, water levels measured were greater than those calculated assuming both methanol and water–gas shift equilibria were attained. Thus, water content was determined from an oxygen balance and accurate measurements of methanol, CO, and CO_2.

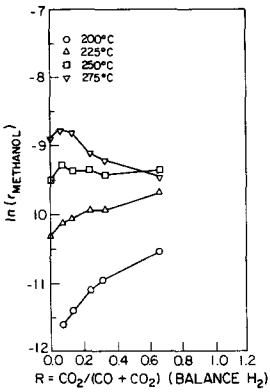

FIG. 4. Effect of temperature and R on the methanol synthesis rate. Cu/ZnO catalyst: $P = 2.41$ MPa, 65% H_2 in feed.

Temperature effect. Figure 4 plots ln r_{MeOH} vs R for 65% H_2 at 2.41 MPa for four temperatures between 200 and 275°C at a space velocity of 37 ml (STP) (g cat.)$^{-1}$ s^{-1}. Below 250°C, the synthesis rate increases with R. At 250°C, however, R has only a slight effect on the synthesis rate, whereas at 275°C, the rate decreases rapidly with R in the range $0.1 < R < 0.66$. Figure 4 is a logarithmic plot of rate. The drop between 0.1 and 0.3 is almost an order of magnitude. This is in good agreement with the data of Klier *et al.* (*25*) for $0.02 < R < 0.3$ and 70% H_2 in the temperature range from 225 to 250°C at 7.5 MPa.

Figure 4 shows a temperature effect on the influence of R not previously observed. An effect of this type would usually be attributed to a change in the rate-controlling step, but since independent routes to methanol from either CO or CO_2 appear to be possible, it could arise from activation energy differences between parallel routes. Conversions at 275°C were greater than those at 225°C, but did not exceed 1.5%. Water in the reactor off-gas accounted for from 0.4 to 0.6%, a range below those reported by Vedage *et al.* (*2*) and Liu *et al.* (*27*) for severe inhibition. Therefore, water inhibition cannot be the explanation of the change in the effect of R on rate shown in the figure.

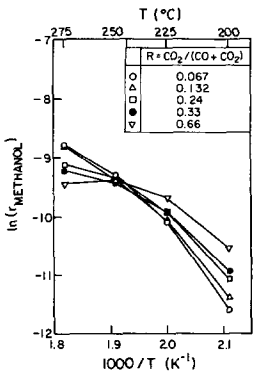

FIG. 5. Arrhenius plots for methanol synthesis as a function of R. Cu/ZnO catalyst: P = 2.41 MPa, 65% H_2 in feed.

Liu *et al.* (*27*) attempted to explain Klier's results in several ways. Their most persuasive argument dealt with water effects. If methanol in Klier's experiments was largely formed from CO_2 rather than CO, water levels at the end of the Klier reactor would reach levels at which strong water inhibition occurs. Liu *et al.* suggest that water activation of the catalyst at low water levels, as reported by Vedage *et al.* (*2*), and inhibition at high values of R, corresponding to higher water levels, explain the Klier results. Our results do not dispute their hypothesis; however, they do suggest that part of the explanation may be due to the effect seen in Fig. 4. The pressure difference, 7.5 MPa vs 2.86 MPa, and differences in catalyst preparation and conditioning may explain the change in the effect of R at temperatures at least 50° below 275°C.

The data on the temperature effect are presented in an Arrhenius plot in Fig. 5 with R as a parameter. The apparent activation energies for the synthesis on the Cu/ZnO catalyst depend on both temperature and R. Nevertheless, the values for $0.067 < R < 0.24$ are in good agreement with published values, which range between 90.8 and 104.6 kJ/mol (*35, 36*). At 65% H_2, Fig. 3 shows about a threefold difference in the rates of methanol synthesis, from CO_2–H_2 and CO–H_2. Thus at R = 0.067 (CO_2 is less than 10% of the carbon oxides), methanol must be formed primarily from CO. The R = 0.067 curve in Fig. 5 shows the least curvature. On the other hand, the most curvature (greatest change in slope, ln r vs $1/T$) occurs for R = 0.33 and 0.66, where both CO and CO_2 are important methanol sources. These considerations suggest that the changing activation energy reflects a change in the importance of the CO and CO_2 sources of methanol. Note that at 275°C, the rate for R = 0.067 is about 10 times the rate at R = 0.66.

Deactivation behavior. Deactivation of the Cu/ZnO catalyst occurred with time-on-stream as noted earlier. To describe this process, experiments were performed at 225°C, 2.86 MPa, and a space velocity of 37 ml g^{-1} s^{-1}. Catalyst samples were exposed for at least 72 h to a feed that was 70% H_2, 23% CO, and 7% N_2 or to a feed of 70% H_2, 23% CO, and 7% CO_2. In both tests, the deactivation was interrupted for periods of 48 or 72 h in which the catalyst was held at 225°C but under N_2. The purpose of the interruption was to see if additional aging processes were at work. Two samples of the Cu/ZnO catalyst were employed, one of which was freshly prepared while the other sample had been reduced for 10 h under H_2, as discussed earlier.

Figure 6 shows the methanol yield for both samples, normalized with respect to the initial yield, as a function of time-on-stream. Freshly prepared catalyst is activated by exposure to the syngas mixture. Although the sample was measured 6 h after the first exposure, it is likely that there is a rapid initial increase in activity, probably in the first hour on stream. Activity continues to increase to a maximum at about 15 h on stream; thereafter it declines relatively slowly.

By contrast, the activity of the H_2-reduced catalyst begins to decline after the first hour on stream. Although Fig. 6 shows that the initial time-on-stream deactivation is more rapid with a feed containing CO_2, a conclusion on the role of CO_2 in deactivation

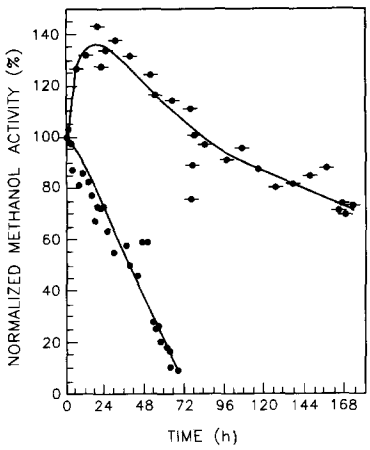

FIG. 6. Deactivation of the Cu/ZnO catalyst with time of exposure to syngas. T = 225°C; P = 2.86 MPa; (—●—) freshly prepared catalyst exposed to 70% H_2, 23% CO, and 7% N_2; (●) reduced catalyst exposed to 70% H_2, 23% CO, and 7% CO_2.

cannot be drawn because of the different pretreatment undergone by the catalyst samples. The line through the data points is not a fit but is intended only to show the data trend. The scattering of the normalized yields indicates, we believe, reproducibility of the measurements.

The sharp drop in yield at about 72 h on stream for the freshly prepared catalyst represents measurements made immediately after resuming syngas flow to the sample after it was held under N_2 for 120 h. Deactivation during this holding period was 30%. The activity is rapidly restored within about a 6-h time-on-stream, so that the net loss due to interruption of the syngas and substitution of nitrogen was negligible. We speculate that the drop and the restoration of activity result from adjustment of the Cu/Zn composition of the surface. Sensitivity of surface composition to the gas-phase composition is noted further on and has been reported in the literature (*7, 24*). Reversibility of the enrichment or depletion of surface metals has been observed.

An interruption in the catalyst exposure to syngas was made for the second sample shown in Fig. 6 after 43 h on stream. In this case, there was no loss of activity even though the catalyst was held under a N_2 atmosphere for 48 h. Instead, there was about a 10% temporary increase in activity; thereafter deactivation occurred at about the same rate. Methane production surged for about a 10-h period after the interruption. We are unable to account for this behavior. We note that this catalyst was exposed to a CO_2-containing feed.

The methane behavior is not shown on the figure but it is nevertheless remarkable. A burst of methane production occurs when the freshly prepared catalyst is exposed to the syngas feed mixture, but this drops to essentially zero within 24 h on stream. For the catalyst sample reduced with H_2, there is also a burst of H_2 production on the first exposure to syngas. This increase occurs during the first hour on stream but then declines until, after 12 h, methane production ceases. Methane formation nevertheless remains much less than methanol formation during this initial period. A possible explanation for the methane surge is flooding of the reduced, possibly Cu crystallites on the catalyst surface by H adatoms. Duprez *et al.* (*7*) quote a doctoral dissertation that claims that ZnO can store hydrogen. The hydrogen species, they claim, is highly mobile and can spill over to the Cu crystallites dispersed in the zinc phase. We speculate that some of this hydrogen reduces the adsorbed oxycarbons to methane as well as forming methanol, the dominant product.

Klier *et al.* (*25*) reported continuous deactivation of their Cu/ZnO catalyst in a CO_2-free syngas mixture, but Kung's group (*27*) observed that a steady state was reached after about a 60% loss of activity.

Surface alteration with exposure to syngas. Activity loss for the methanol synthesis catalyst is usually attributed to sulfur poisoning, depletion of Cu from the surface, sintering or agglomeration of Cu crystallites in a ZnO matrix, or to copper overreduction (*12, 25*). Sulfur can be rejected as a source, because the feed gases were sulfur-free. To explore the remaining explanations, X-ray

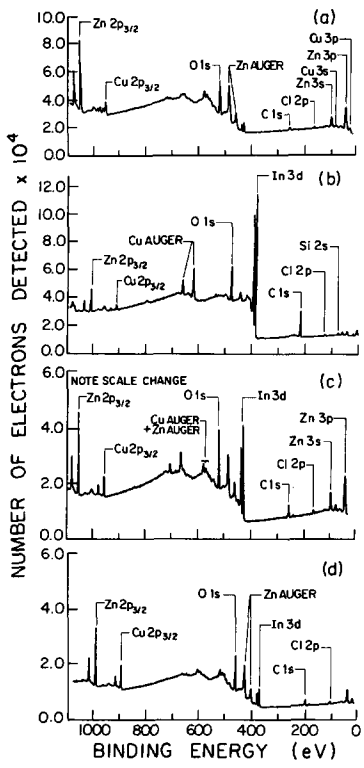

FIG. 7. X-ray photoelectron and Auger spectra for Cu/ZnO catalyst. (a) Freshly prepared, (b) reduced in H_2 at 250°C for 10 h, (c) reduced and exposed to 65% H_2, 35% CO, (d) reduced and exposed to 65% H_2, 35% CO_2.

photoelectron (XPS) and Auger spectroscopy measurements were made on catalyst samples on our behalf by the Surface Science Laboratory of the University of Western Ontario. The results presented below are drawn from their report (*30*). Catalysts sent to their laboratory were loaded into clean glass vials using an N_2 glove bag and were maintained under N_2 pressure until use. Spectra were obtained from catalyst samples pressed into an indium foil. A separate set of samples was used, so the relation to deactivation behavior is by inference. An Al$K\alpha$ X-ray photon excitation source ($h\nu$ = 1486.6 ev) was employed to obtain the Cu,Zn $2p_{3/2}$ photoelectron lines as well as the Cu (LMM) Auger lines. Figure 7 shows the XPS spectra obtained for the four Cu/ZnO samples and the Auger spectra. Peaks are identified from literature data relative to the C 1*s* line and the relative amounts of zinc and copper on the surface were determined from the respective $2p_{3/2}$ peaks. The oxidation state of the copper was determined from the Auger α parameter on the basis of a 2-eV shift between Cu^{2+} and Cu^{+}. The presence of Cu shakeup satellite peaks of approximately 40% of the intensity of the Cu $2p_{3/2}$ line indicated Cu presence as Cu^{2+}.

Comparison of the Zn and Cu $2p_{3/2}$ intensities indicates a low ratio of Cu : Zn on the surface in spectra (a) for a freshly prepared catalyst. Despite the low intensities, the satellite peaks for Cu $2p_{3/2}$ and for Cu $2p_{1/2}$ are clearly evident at about 40% intensity. These satellite peaks disappear in the spectra for the reduced catalysts; namely (b) prior to use; (c) exposed for an extended period to CO–H_2; or (d) exposed for an extended period to CO_2–H_2. A 65 : 35% H_2 : CO_2 mixture did not reoxidize the catalyst to Cu^{2+} to any detectable extent. Comparison of the $2p_{3/2}$ intensities shows, however, that the CO_2–H_2 feed brought the surface Cu to its level in the bulk of the catalyst. Low surface levels of Cu have been observed (*37*) and the role of CO_2 in drawing Cu to the surface is discussed by Menon and Prasada Rao (*38*).

The shift of the Auger α parameter for the Auger data led to the assignment of Cu^{+} for Cu on the surface. This observation does not agree with the literature. Syngas exposure results in Cu metal (*39*) or a mixture of Cu and Cu^{+} on the surface. Constancy of the Auger α for Zn indicates Zn remains as ZnO regardless of the gas environment.

The carbon 1*s* line is not intense in the freshly prepared catalyst sample, but increases substantially in spectrum (b) for the sample reduced in hydrogen. Because this sample has not been exposed to syngas, we believe that the C 1*s* line must be due to contamination during handling of the sample. The line intensity decreases in spectra (c) and (d). Contamination is probably responsible for the Cl 2*p* line also present in

TABLE 2

XPS Results on Surface Composition of the Cu/ZnO Catalyst in Various Stages of Usage

	C1[a]	C2[b]	C3[c]	C4[d]
Cu : Zn[e] (atomic ratio)	16 : 84	21.3 : 78.7	20 : 80	30 : 70
Binding energy of Cu, $2p_{3/2}$[f] (eV)	933.4	932.14	932.5	932.79
Auger parameter of Cu, α[g] (eV)	364.8	362.8	362.6	362.6
Percentage of total Cu in a particular oxidation state	100% Cu^{+2} mostly CuO	100% Cu^{+1} Cu_2O	100% Cu^{+1} Cu_2O	100% Cu^{+1} Cu_2O
Binding energy of Zn $2p_{3/2}$[e] (eV)	1021.9	1021.5	1021.9	1022.1
Auger parameter of Zn, α[g] (eV)	523.5	523.3	523.4	523.3

[a] Unreduced/unused catalyst.
[b] Reduced/unused catalyst.
[c] Reduced and used catalyst. Exposed finally to a steady-state feed gas mixture, H_2/CO (65/35 mol%).
[d] Reduced and used catalyst. Exposed finally to a steady-state feed gas mixture, H_2/CO_2 (65/35 mol%).
[e] Bulk elemental composition Cu : Zn = 30.97 : 69.03 atomic ratio.
[f] References to carbon 1*s* = 285.0 eV.
[g] α = K.E. of Auger electron − K.E. of photoelectron (1486.6 eV).

all spectra. Table 2 summarizes the XPS study performed for us. Exposure of the samples was done *in situ*.

The lack of change in the Cu : Zn ratio between the reduced catalysts and one that has had prolonged exposure to syngas suggests that deactivation of the Cu/ZnO catalyst is not due to the Cu : Zn ratio on the surface. The Auger results indicate that for this catalyst preparation and conditioning in hydrogen, surface copper is predominantly Cu^+ regardless of the exposure to either $CO–H_2$ or $CO_2–H_2$ (in a 35 : 65% ratio). Consequently, deactivation is not the result of reduction to the metal. If metallization did occur, increased methane formation would be anticipated. Methane was not formed on this catalyst. We speculate that deactivation occurs through agglomeration (growth) of the copper crystallites reducing the $Cu_2O–ZnO$ synergism.

Cu/ZnO/Al$_2$O$_3$ Catalyst

Kinetics. Methanol synthesis on this catalyst differs from synthesis on the binary Cu/ZnO in several aspects: the ternary catalyst is more active, the R vs % H_2 interaction is somewhat different, and a small amount of methane is formed.

Methanol production as a function of R, the CO_2 fraction in the carbon oxide portion of the feed, appears in Fig. 8 for this catalyst. Rates of production are shown for four levels of H_2 in the feed. A comparison with Fig. 2 shows that the rates are about 30% greater for the $Cu/ZnO/Al_2O_3$ catalyst at each % H_2. Increasing the hydrogen partial pressure in the feed mixture increases the synthesis rate. In general, the rate also increases with the increasing CO_2 content of the feed mixture. With the ternary catalyst, at the lowest % H_2, the influence of CO_2 on the rate rises rapidly to $R \approx 0.4$; thereafter, increasing the CO_2 content does not seem to affect the methanol production rate. This was not seen for the Cu/ZnO catalyst.

Figure 9 isolates the experiments using either CO or CO_2 alone in the feed stream from the data in Fig. 8. As in Fig. 3, there is a fivefold rate difference between CO- and

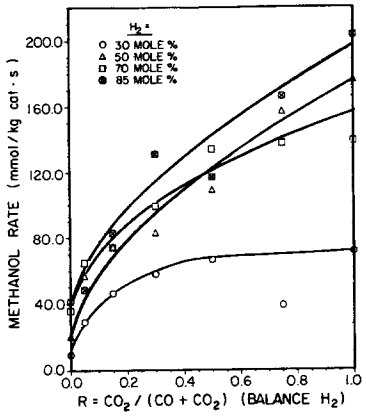

FIG. 8. Methanol synthesis rate as a function of R and % H_2. Feed contains CO, CO_2, and H_2; T = 225°C; P = 2.86 MPa; flow = 14.8 ml (STP) s^{-1}; $Cu/ZnO/Al_2O_3$ catalyst.

CO_2-containing feeds at high values of % H_2. These two figures clearly indicate independent routes from CO and CO_2 to methanol.

The $Cu/ZnO/Al_2O_3$ catalyst produces methane as a minor product, roughly 5 to 10% of the yield of methanol. Methane formation is not usually observed for this catalyst (*35, 36, 40*). Only Nappi *et al.* (*41*) report CH_4, but their catalyst was prepared from the same precursors used in this study. It is possible that methane arises from iron impurities in the Al_2O_3 used to prepare our catalyst. The rate of methane formation is proportional to the H_2 partial pressure and varies with the CO_2 content of the feed as may be seen in Fig. 10. Because of trace amounts of methane present in the CO cylinders used, the experimental data were corrected for this contribution. Inaccuracies in the measurements or very small variation in the trace methane led in some cases to negative values of the rate of methane formation seen in the figure. This occurred only at low ratios of hydrogen to carbon oxides. Methane content was not measured for all cylinders. Figure 10 suggests that methane is not formed unless the hydrogen content of the feed exceeds 30%. At higher levels, the production rate appears proportional to the hydrogen partial pressure, following the relation $(y_{H_2} - 0.3)^{1.5}$. The figure also shows the methane yield increasing with R up to 0.75. The rate, however, is less for a H_2/CO_2 mixture. Unfortunately, our data do not indicate the value of R at which the methane yield decreases. The dashed line in the figure connects the data points for the appropriate % H_2.

A comparison of Fig. 10 with Fig. 8 shows that up to R = 0.75 the methane and methanol rates increase more or less proportionally. Clearly CO_2 cannot be a diluent for methane formation. One interpretation of the parallel rates of formation would be that methane and methanol are formed at the

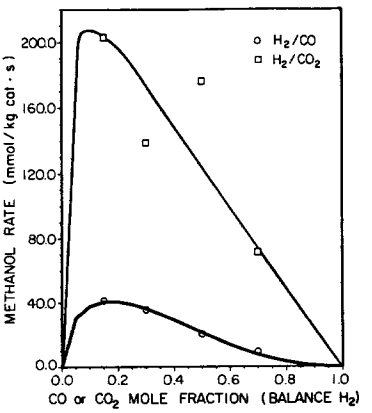

FIG. 9. Methanol synthesis rate for CO/H_2 and CO_2/H_2 feeds. T = 225°C; P = 2.86 MPa; flow = 14.8 ml (STP) s^{-1}; $Cu/ZnO/Al_2O_3$ catalyst.

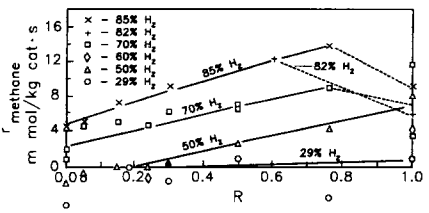

FIG. 10. Methane formation rate for $Cu/ZnO/Al_2O_3$ catalyst. T = 225°C; P = 2.86 MPa; flow = 14.8 ml (STP) s^{-1}; $Cu/ZnO/Al_2O_3$ catalyst.

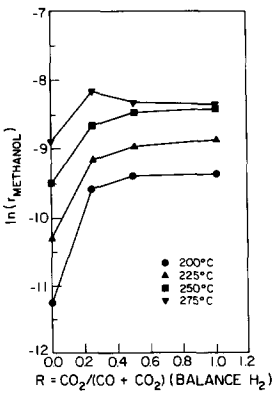

FIG. 11. Effect of temperature and R on the methanol synthesis rate. Cu/ZnO/Al_2O_3 catalyst: P = 2.86 MPA; 70% H_2 in feed.

same catalytic sites, if indeed methane does not result from impurities in the alumina used.

Temperature effect. Comparison of Fig. 11 for the Cu/ZnO/Al_2O_3 catalyst to Fig. 4 for the Cu/ZnO catalyst indicates different behaviors. The synthesis rate increases initially as R increases for all four temperatures used. At 275°C, the rate becomes constant at higher R, however, Moreover, the slope of the ln r vs R curves drops as temperature increases, suggesting that at a sufficiently elevated temperature, the effect of R vanishes and the rate may even decrease as the fraction of CO_2 in the carbon oxide feed increases. Indeed, judging from the data at 275°C, this temperature may be under 300°C. Conditions for Fig. 11 differ slightly from those in Fig. 4: reactor pressure was 2.86 MPa and 70% H_2 was used in the feed. Chinchen *et al.* (*12*) argue from ^{14}C labeling experiments at about 5 MPa and 250°C that methanol arises predominantly from CO_2 for this ternary catalyst. Figure 11 suggests that at higher temperatures the role of CO as a methanol source becomes more important.

The data of Fig. 11 are replotted as an Arrhenius plot in Fig. 12. Just as for the Cu/ZnO catalyst, the activation energy is a function of R and temperature. However, with the Cu/ZnO/Al_2O_3 catalyst, activation energy changes little with increasing temperature with a CO/H_2 syngas mixture.

Addition of CO_2 to give $R > 0$ causes a fall in activation energy and a decrease in this parameter as temperature increases. At 275°, the rate of methanol synthesis becomes independent of R (see Fig. 12). For the Cu/ZnO catalyst, this is observed at about 250°C (Fig. 5). Activation energy at R = 0 was found to be 75 kJ/mol methanol, whereas at R = 1, it was 39 kJ/mol. Activation energies at R = 0.23 and 0.50 were 34 to 35 kJ/mol, quite close to the value for a CO_2/H_2 syngas. These observations support the contention of Chinchen *et al.* (*4*) that the reaction through CO_2 dominates methanol formation from CO–CO_2 mixtures.

Deactivation behavior. Deactivation was observed for the same gas mixtures, temperatures, and space velocities employed with the Cu/ZnO samples. However, for the ternary catalyst, both catalyst samples were conditioned in flowing hydrogen for 10 h at 225°C. Figure 13 shows the loss of methanol activity with time-on-stream for the two samples. These tests were not interrupted. Clearly, the presence of CO_2 in the syngas mixture moderates the deactivation so that the rate of activity loss is about half of the rate at 70% H_2 and 23% CO with CO_2 absent from the feed. After 72 h on stream, the activity loss is 35% with CO_2 in the feed

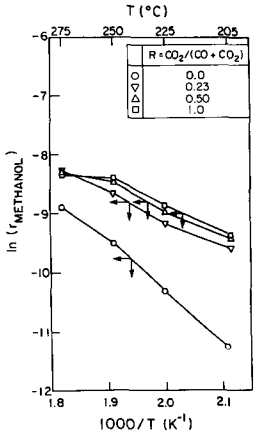

FIG. 12. Arrhenius plots for methanol synthesis as a function of R. Cu/ZnO/Al_2O_3 catalyst: P = 2.86 MPa, 70% H_2 in feed.

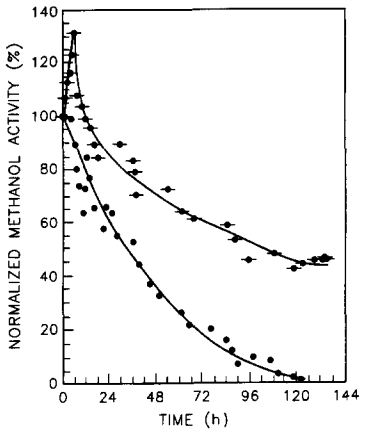

FIG. 13. Deactivation of the $Cu/ZnO/Al_2O_3$ catalyst for methanol synthesis with time of exposure to syngas. T = 225°C; P = 2.86 MPa; (—●—) reduced catalyst exposed to 70% H_2, 23% CO, and 7% N_2; (●) reduced catalyst exposed to 70% H_2, 23% CO, and 7% CO_2.

vs 80% in its absence. Moreover, with CO_2 present, the $Cu/ZnO/Al_2O_3$ catalyst undergoes a 30% activation in the first 6 h on stream. Only after this period does deactivation commence.

Comparison of the deactivation data of Figs. 6 and 13 shows further differences between the binary and ternary catalyst. The initial (t = 0) activity of the ternary catalyst is about 65% greater when CO_2 is present (although this is not evident from the figures, which show activity normalized with respect to time zero). Over 72 h, the binary catalyst with CO_2 present loses 90% of its initial activity (lower curve in Fig. 6), whereas the ternary catalyst loses just 35% (upper curve in Fig. 13). Exposure of the hydrogen-conditioned binary catalyst to the CO_2-rich syngas furthermore does not increase its activity.

As observed with Cu/ZnO, exposure of the hydrogen-conditioned ternary catalyst to syngas causes an initial burst of methane production regardless of the presence or absence of CO_2 in the feed gas (Fig. 14). Excess methane formation falls rapidly over ca. 6 h when CO_2 is present; in its absence it persists for 6 h, before tailing off in the next 6 h. Methane formation, initially some 10% of methanol formation, drops in parallel with methanol formation with the CO_2-free syngas, whereas with CO_2 present, it drops over 6 h to ca. 5% of methanol formation and then follows the methanol behavior as a comparison of Figs. 13 and 14 shows.

Surface alteration with exposure to syngas. The surface analysis techniques discussed earlier for the binary catalyst were applied to three samples of the $Cu/ZnO/Al_2O_3$ catalyst.: (1) a freshly prepared, unused sample; (2) a sample reduced in H_2 but unused; and (3) a sample used in both steady-state and cycling experiments with and without CO_2. The spectra obtained are collected in Fig. 15. Spectrum (a) for the fresh sample confirms that copper is present primarily as Cu^{2+}; however, the relative magnitudes of the Cu and Zn $2p_{3/2}$ peaks indicate surface depletion in Cu. Other spectral data suggest Al depletion in addition. On reduction in H_2 for 10 h at 225°C, the value of the Auger α for Cu suggests partial reduction of the surface Cu to Cu^+. The relative intensities of the Cu and Zn $2p_{3/2}$ lines in (b) indicate further depletion of Cu in the surface. There is little change between

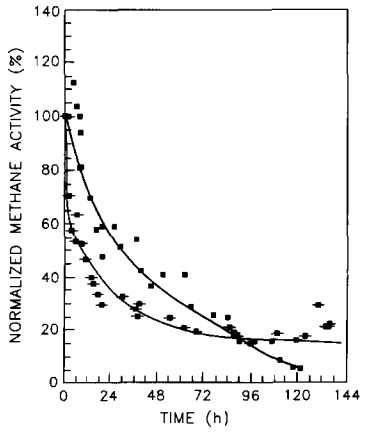

FIG. 14. Deactivation of the $Cu/ZnO/Al_2O_3$ catalyst for methane synthesis with time of exposure to syngas. T = 225°C; P = 2.86 MPa; (—■—) reduced catalyst exposed to 70% H_2, 23% CO, and 7% N_2; (■) reduced catalyst exposed to 70% H_2, 23% CO, and 7% CO_2.

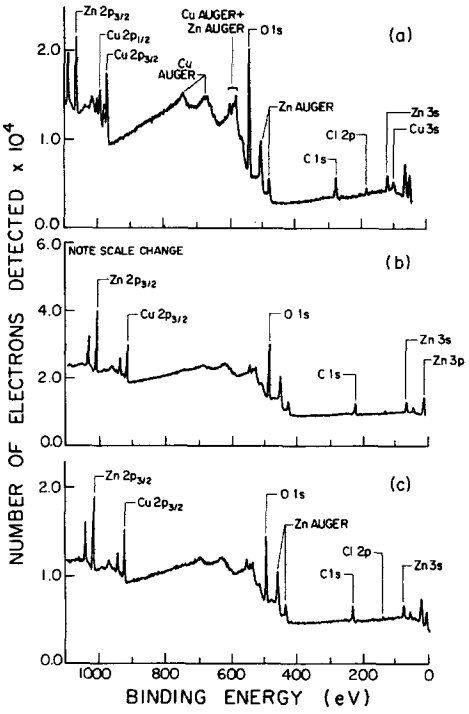

FIG. 15. X-ray photoelectron spectra for Cu/ZnO/Al_2O_3 catalyst. (a) Freshly prepared, (b) reduced in H_2 at 250°C for 10 h, (c) reduced and exposed to various CO–CO_2–H_2 mixtures.

spectra (b) and (c) so that exposure of the ternary catalyst to various syngas mixtures does not alter surface composition or the oxidation state of Cu substantially. The Auger α measurement for Cu, however, suggests that no Cu^{2+} is present in the catalyst surface.

Results of the XPS study of the Cu/ZnO/Al_2O_3 catalyst are summarized in Table 3. The carbon peaks in Fig. 15 spectra are not significant. The relative intensities of the C 1*s* peaks are about the same for samples (1) to (3) even though the first two samples were not exposed to syngas; thus, these carbon readings arise from contamination. In all the ternary catalyst surface measurements, Cu content is greater than for the binary catalyst. This difference may account for the higher activity of the alumina-containing catalyst. The latter catalyst is clearly more difficult to reduce and the higher level of the Cu^{2+} (see Table 3) could explain the higher initial activity of the ternary catalyst when both catalyst go on stream.

DISCUSSION

Role of the Water–Gas Shift

If methanol is formed only via CO_2, as suggested by Chinchen *et al.* (*4*) for some catalysts, or only via CO, as Klier and coworkers (*2*) claim, the water–gas shift (WGS) must occur when $0 < R < 1$. Data obtained in this study allowed an examination of how completely the shift is achieved. The extent of the shift could be measured by comparing the experimentally determined CO/CO_2 mole ratio or mole fraction to the ratio calculated from the known H_2 mole fraction and the measured water vapor mole fraction. This is done in Figs. 16 and 17. Measuring water vapor chromatographically using a TCD detector was inaccurate because of the low conversions in the experiments. Consequently, water was estimated from an oxygen balance using the much more accurately measured CO, CO_2, and methanol concentrations. This procedure correlates errors in the measured CO/CO_2 ratio with variations in the equilibrium ratio; this undoubtedly accounts for much of the scatter in Figs. 16 and 17.

Figure 16 includes data for both catalysts studied and suggests that for most of the measurements, the shift proceeds to equilibrium. The solid line in the figure is not a fitted line, but shows the equality condition. With the exception of points at experimental CO/CO_2 ratios of 17, 23–26, and 31, the equality condition (meaning full attainment of equilibrium) is achieved.

Figure 16 does not resolve satisfactorily the experimental data for CO/CO_2 ratios below 2. These data are examined in Fig. 17, in which the achievement of equilibrium, expressed as the quotient of $(CO/CO_2)_{experimental}$ and $(CO/CO_2)_{equilibrium}$, is plotted against the measured mole fraction of carbon monoxide leaving the reactor. The equilibrium condition is represented by a

TABLE 3

XPS Results on Surface Composition of the $Cu/ZnO/Al_2O_3$ Catalyst in Various Stages of Usage

Cu : Zn : Al[d] (mole%)	41.3 : 51.7 : 7.0	32.4 : 57.8 : 9.8	31.7 : 57.6 : 10.7
Binding energy of Cu, $2p_{3/2}$[e] (eV)	933.65	932.72	932.65
Auger parameter of Cu, α[f] (eV)	—	362.9	362.74
Percent of total Cu in a particular oxidation state	100% Cu^{+2} CuO	20% Cu^{+1} 80% Cu^{+2} Cu_2O; CuO	100% Cu^{+1} Cu_2O
Binding energy of Zn, $2p_{3/2}$[e] (eV)	1022.16	1022.29	1022.37
Auger parameter of Zn, α[f] (eV)	522.89	523.08	523.14

[a] Unreduced/unused catalyst.
[b] Reduced/unused catalyst
[c] Reduced/used in cycling experiments (pulsing of a syngas feed with CO_2 doses).
[d] Bulk elemental composition, Cu : Zn : Al = 59.5 : 31.9 : 8.6 (atomic ratio).
[e] Referenced to carbon 1s = 285.0 eV.
[f] α = K.E. of Auger electron − K.E. of photoelectron (1486.6 eV).

quotient of unity. This plot shows, however, that the WGS equilibrium is not attained for $y_{CO} < 0.05$. Indeed, Fig. 17 indicates that the shift does not proceed at all for CO_2–H_2 syngas mixtures over either catalyst. The reason for this surprising but clearly substantiated observation is not known. Figures 3 and 9 show that methanol is formed so that a WGS component, namely water, is present even though its mole fraction does not exceed 0.01. Only CO is absent. Perhaps this component must be present for the WGS to proceed. The shift reaction occurs, even though equilibrium is not reached for $0 < y_{CO} < 0.05$.

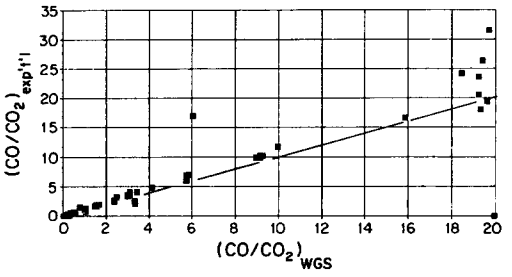

FIG. 16. Test of the reverse water–gas shift equilibrium for both catalysts.

The absence of the WGS is further evidence that separate pathways from CO_2 to methanol and from CO to methanol must exist. The shift reaction cannot occur for CO–H_2 syngas mixtures. Nonetheless, the WGS could be involved in methanol synthesis for $0.05 < R < 0.95$, since our experiments indicate equilibrium is reached.

Activation Energy

Although the variation of the measured activation energy with R and temperature seen in Figs. 5 and 12 has not been reported earlier, this behavior is anticipated by kinetic models for methanol synthesis such as those offered by Kuznetsov *et al.* (*42*) and Villa *et al.* (*40*) for binary catalyst, and by Graaf *et al.* (*43*) for ternary catalysts. These models all contain denominator terms involving products of temperature-dependent parameters and concentrations of CO or CO_2.

The significance of these Arrhenius plots is with respect to the synthesis mechanism. The decreasing slopes in the ln r vs $1/T$ plots as R and T increase suggest that methanol cannot be formed exclusively by separate

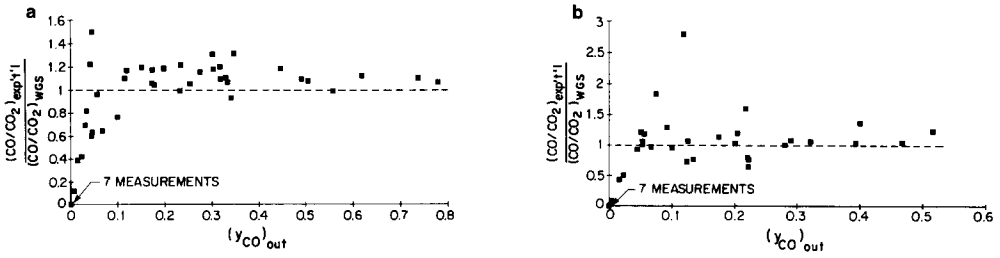

FIG. 17. Variation of attainment of the reverse water–gas shift equilibrium as a function of outlet CO mol fraction: (a) Cu/ZnO catalyst, (b) $Cu/ZnO/Al_2O_3$ catalyst.

pathways from CO and from CO_2. Activation energies for the separate reactions are quite different (Fig. 12), as various authors demonstrate. If methanol formation from CO_2 and CO is additive, then at high temperatures the measured activation energy should approach the higher activation energy (for the CO → methanol reaction) while at lower temperatures, the measured E should become the lower activation energy (for the CO_2 → methanol reaction). Thus, ln r vs $1/T$ should be concave upward. However, the plots in Figs. 5 and 12 are convex or concave downward.

Catalyst particle size and space velocity were chosen to be well away from values where transport interference arises using the highest rates measured at 90% H_2 and 225°C. Therefore, it is unlikely that transport interference is a significant factor at 275°C as the rate increase between these temperatures never exceeds fivefold. Therefore, the Arrhenius plots seem to indicate the occurrence of either a decrease in turnover number or a decrease in sites for CO_2 conversion to methanol between 225 and 250°C for Cu/ZnO and above 250°C for the $Cu/ZnO/Al_2O_3$ catalyst. Alternatively, a change in mechanism must occur with a significant reduction in the activation energy. Our data allow no further insight as to what happens.

Deactivation differences, methanol formation, and the sensitivity of activation energy to the Cu/Zn ratio and/or the presence of Al_2O_3 suggests that catalyst preparation and perhaps purity of materials influences the participation of CO and CO_2 in methanol synthesis. Perhaps these factors influence the temperature at which the synthesis from CO_2 loses importance as illustrated by the measurements presented in Figs. 4 and 11 for the two catalysts examined in this study. This temperature dependence of the relative participation of CO and CO_2 in methanol synthesis may be a better explanation of the widely different experimental results obtained by Klier *et al.* (*25*) and Liu *et al.* (*5*) than the explanation of water inhibition suggested by earlier investigators.

CONCLUSIONS

Measurements of methanol formation rates at different synthesis gas compositions and temperatures confirm many earlier studies, which indicate that methanol can be formed from either CO or CO_2. When both reactants are present in the syngas, the rates from either reactant are additive, with a further contribution to methanol arising from interconversion, mainly CO to CO_2, via the water–gas shift, utilizing water formed in the methanol synthesis. However, the water–gas shift on both the Cu/ZnO and $Cu/ZnO/Al_2O_3$ catalysts does not proceed for a CO_2/H_2 syngas. A CO level above 5% seems necessary for the WGS to proceed to equilibrium. At temperatures greater than 225°C, formation of methanol from CO_2 decreases over the Cu/ZnO catalyst, whereas a temperature above 250°C is needed to effect the formation of methanol from CO_2 on the ternary $Cu/ZnO/Al_2O_3$ catalyst.

ACKNOWLEDGMENTS

Studies reported in this contribution were supported by operating grants from the Natural Sciences and Engineering Research Council of Canada to the principal investigators (P.L.S. and R.R.H.). We also acknowledge helpful discussions with Professor Y. Amenomiya.

REFERENCES

1. Rozovskii, A. Ya., *Kinet. Katal.* **21,** 97 (1980).
2. Vedage, G. A., Pitchai, R., Herman, R. G., and Klier, K., *in* "Proceedings, 8th International Congress on Catalysis, Berlin 1984," Vol. II, p. 47. Dechema, Frankfurt-am-Main, 1984.
3. Kinnaird, S., Webb, G., and Chinchen, G. C., *J. Chem. Soc. Faraday Trans.* **83,** 3399 (1987).
4. Chinchen, G. C., Denny, P. J., Parker, D. G., Spencer, M. S., and Whan, D. A., *Appl. Catal.* **30,** 333 (1987).
5. Liu, G., Willcox, D., Garland, M., and Kung, H. H., *J. Catal.* **96,** 251 (1985).
6. Jackson, S. D., *J. Catal.* **115,** 247 (1989).
7. Duprez, D., Fevhat-Hamida, Z., and Bettahar, M. M., *J. Catal.* **124,** 1 (1990).
8. Okamoto, Y., Fukino, K., Imanaka, T., and Teranishi, S., *in* "Proceedings, 8th International Congress on Catalysis, Berlin, 1984" Vol. V, p. 59. Dechema, Frankfurt-am-Main, 1984.
9. Fleisch, T. H., and Mieville, R. L., *J. Catal.* **90,** 165 (1984).
10. Vlaic, G., Bart, J. C. J., Cavigiolo, W., and Mobilio, S., *Chem. Phys. Lett.* **76,** 543 (1980).
11. Monnier, J. R., Apai, G., and Hanrahan, M. J., *J. Catal.* **88,** 523 (1984).
12. Chinchen, G. C., Waugh, K. C., and Whan, D. A., *Appl. Catal.* **25,** 101 (1986).
13. Chinchen, G. C., Denny, P. S., Parker, D. G., Short, G. D., Spencer, M. S., and Waugh, K. C., *Prep. Pap.—Am. Chem. Soc., Div. Fuel Chem.* (1984).
14. Tagawa, T., Pleizer, G., and Amenomiya, Y., *Appl. Catal.* **18,** 285 (1985).
15. Bowker, M., Houghton, H., and Waugh, K. C., *J. Chem. Soc. Faraday Trans.* **77,** 3023 (1981).
16. Deluzarche, A., Kieffer, R., and Muth, A., *Tetrahedron Lett.* **38,** 3357 (1977).
17. Deluzarche, A., Hindermann, J. P., and Kieffer, R., *J. Chem. Res.* **72,** 934 (1981).
18. Ramaroson, E., Kieffer, R., and Kiennemann, A., *Appl. Catal.* **4,** 281 (1982).
19. Saussey, J., Lavalley, J. C., Lamotte, J., and Rais, T., *J. Chem. Soc. Chem. Commun.* **5,** 278 (1982).
20. Amenomiya, Y., and Tagawa, T., *in* "Proceedings, 8th International Congress on Catalysis, Berlin, 1984" Vol. II, p. 557. Dechema, Frankfurt-am-Main, 1984.
21. Edwards, J. F., and Schrader, G. L., *Appl. Spectrosc.* **35,** 559 (1981).
22. Edwards, J. F., and Schrader, G. L., *J. Phys. Chem.* **88,** 5620 (1984).
23. Edwards, J. F., and Schrader, G. L., *J. Phys. Chem.* **89,** 782 (1985).
24. Denise, B., Sneeden, R. P. A., Beguin, B., and Cherifi, O., *Appl. Catal.* **30,** 353 (1987).
25. Klier, K., Chatikavanij, V., Herman, R. G., and Simmons, G. W., *J. Catal.* **74,** 343 (1982).
26. Rozovskii, A. Ya., Kagan, Yu. B., Lin, G. I., Slivinskii, E. V., Loktev, S. M., Liberov, L. G., and Bashkirov, A. N., *Kinet. Katal.* **17,** 1314 (1976).
27. Liu, G., Willcox, D., Garland, M., and Kung, H. H., *J. Catal.* **90,** 139 (1984).
28. Kieffer, R., Ramaroson, E., Deluzarche, A., and Trambouze, Y., *React. Kinet. Catal. Lett.* **16,** 207 (1981).
29. Denise, B,. Sneeden, R. P. A., and Hamon, C., *J. Mol. Catal.* **17,** 359 (1982).
30. Chanchlani, K., Ph.D. thesis, Department of Chemical Engineering, University of Waterloo, Ontario, Canada, 1988.
31. Dietz, W. A., *J. Gas Chromat.* **5,** 68 (1967).
32. Klier, K., and Herman, R. G., "Methanol and Methyl Fuel Catalysts," Final Technical Report prepared for US DOE under contract ET-78-S-01-3177, 1980.
33. Butt, J. B., and Weekman, V. W., *AIChE Symp. Ser.* **70,** 27 (1974).
34. Chinchen, G. C., Mansfield, K., and Spencer, M. S., *CHEMTECH.* **Nov.,** 692 (1990).
35. Leonev, V. E., Karabaev, M. M., Tsybina, E. N., and Petrishcheva, G. S., *Kinet. Katal.* **14,** 970 (1973); **14,** 848 (1973). [in English]
36. Agny, R. M., and Takoudis, C. G., *Ind. Eng. Chem. Prod. Res. Dev.* **24,** 50 (1985).
37. Petrini, G., and Garbassi, F., *Actas Simp. Iberoam. Catal., 9th* **2,** 918 (1984).
38. Menon, P. G., and Prasada Rao, T. S. R., *Catal. Rev.-Sci. Eng.* **20,** 97 (1979).
39. Okamoto, Y., Fukino, K., Imanaka, T., and Teranishi, S., *J. Chem. Soc., Chem. Commun.* **24,** 1405 (1982).
40. Villa, P., Forzatti, P., Buzzi-Ferraris, G., Garone, G., and Pasquon, I., *Ind. Eng. Chem. Process Des. Dev.* **24,** 12 (1985).
41. Nappi, A. O., Fabbricino, L., Hudgins, R. R., and Silveston, P. L., *Can. J. Chem. Eng.* **63,** 963 (1985).
42. Kuznetsov, V. D., Shub, F. S., and Temkin, M. I., *Kinet. Katal.* **25,** 606 (1984); **25,** 510 (1984). [in English]
43. Graaf, G. H., Stamhuis, E. J., and Beenackers, A. A. C., *Chem. Eng. Sci* **43,** 3185 (1989).